

DETERMINATION OF VAPOR BUBBLE DIAMETER OF FC3284, FC84 AND THEIR BINARY MIXTURES DURING POOL BOILING

C. Kerem Ceylan¹, Olaf Koeppen², Sebiha Yildiz¹

¹Yildiz Technical University, Mechanical Engineering Department, Heat and Thermodynamics Division, 34349 Besiktas /Istanbul/Turkey

²TU-Berlin, Institut für Energietechnik, KT2, Marchstr. 18, 10587 Berlin, Germany

syildiz@yildiz.edu.tr

o.koeppen@tu-berlin.de

ABSTRACT

The bubble diameter of FC3284, FC84 and their mixtures during pool boiling were measured with a dual-probe which was located at a certain distance from the heating surface. In this study, temperature controlled heating surface was used. The difference between heating surface and saturation temperatures was increased gradually to obtain entire pool boiling regions at atmospheric pressure. Along the entire boiling curve, vapor bubble diameter was determined at that specified point. First of all, bubble diameter was determined for pure substances and their binary mixtures respectively. Different bubble diameters were determined in the different pool boiling regions. The results were compared with each other and with existing correlations in literature. It was found out that surface tension, viscosity and wall superheat are important factors which may affect the bubble departure diameter. At the beginning of the nucleate boiling, the results were in agreement with some related correlations in the literature and bubble diameters for pure substances FC3284 and FC84 were lower when compared to that of their binary mixtures.

INTRODUCTION

Boiling has numerous applications in industry such as refrigeration, power generation, chemical processing and nuclear reactors. However, physical phenomenon of pool boiling has not been completely understood yet. For this reason, bubble dynamics is important for evaluating boiling characteristics. Bubble diameter plays a significant role in boiling regions and may affect the bubble dynamics on heating surface and at any distance from the heating surface. The correlations, which have been developed for bubble diameter in literature so far, are valid only for departure diameter. Therefore, there is a need for studies investigating the difference between experimental and theoretical bubble diameters at a certain distance from the heating surface and in the different pool boiling regions. In this study, the measured bubble diameter was compared with some correlations for departure diameter.

NOMENCLATURE

C_p	[J/kg.K]	Specific heat flux
d_b, d_B	[m]	Bubble diameter
d_{bd}	[m]	Departure diameter of bubble
g	[m/s ²]	Gravitational acceleration
Δh_v	[J/kg]	Latent heat of vaporization
Ja	[-]	Jacob number
k	[W/m.K]	Thermal conductivity
M	[g/mol]	Molecular weight
Pr	[-]	Prandtl number
q^*	[-]	Relative heat flux
T	[K]	Temperature
ΔT_s	[K]	Wall superheat
t	[s]	Time

Greek

Symbols

θ	[°]	Contact angle
μ	[Pa.s]	Dynamic viscosity
ρ	[kg/m ³]	Density
σ	[N/m]	Surface tension

Subscripts

I	Inlet
l	Liquid
O	Outlet
s	Saturation
v	Vapor
w	wall

Departure diameter

The departure diameter is the diameter of the vapor bubble when the bubble detaches from the heater surface. The sum of the buoyancy forces and dynamic forces increases faster with the bubble radius than the adhesive forces that hold the vapor bubble on the surface. Therefore, the bubble starts to depart from the heating surface after reaching a certain bubble diameter value. The main parameters that affect the bubble departure diameter are pronounced generally as contact angle, surface roughness, surface tension, wall superheat, pressure, gravity, density and viscosity.

In the study of S. Hamzekhani et al. [1], bubble departure diameters of pure water, ethanol and various binary mixtures, including ethanol/water, NaCl/water and Na₂SO₄/water were investigated in saturated pool boiling at atmospheric pressure. The experiments were carried out with a wide range of concentrations. It was observed in the experimental results that bubble diameter increased with increasing heat flux and also electrolyte concentration for all test fluids. However, bubble departure diameter decreased with increasing ethanol mass fraction. H. Sakashita et al. [2] examined bubble departure diameter of 2-propanol/water mixture and they observed that the departure diameter of bubbles decreased by addition of 2-propanol at low heat fluxes. According to [3], the bubble diameter was predominantly influenced by the system pressure and not by the heat flux. In this study, it is not possible to examine the effect of pressure and contact angle, since the system pressure is constant during experiments and the test substances have approximately similar physical properties (FC3284, FC84). Nevertheless, there is a 30 °C difference between their saturation temperatures.

Departure diameter for a vapor bubble was investigated in this study through some equations. One of the most reliable existing models for prediction of the bubble diameter for boiling of pure liquids and also liquid mixtures is proposed by Fritz [4].

It presents a balance of gravity and surface tension forces, taking the effect of contact angle into account.

$$d_{bd} = 0.0208 \theta \sqrt{\frac{\sigma}{g(\rho_l - \rho_v)}} \quad (1)$$

where θ is 35° for mixtures in general and 45° for water.

It should be taken into consideration that the Fritz equation [4] is only valid for low heat flux at the beginning of the nucleate boiling. In other areas of boiling curve, the coalescence of vapor bubbles plays a role and the vapor bubbles are affected by it, especially at higher heat fluxes.

Kutateladze and Gogonin [5] correlated a large amount of data from the literature. They proposed following equations:

$$d_{bd} = 0.25 \sqrt{\frac{\sigma}{g(\rho_l - \rho_v)}} (1 + 10^5 \cdot C)^{\frac{1}{2}} \quad (2)$$

$$C = \frac{Ja}{Pr_l} \left[\frac{\mu_l^2}{g \rho_l (\rho_l - \rho_v)} \right] \left[\frac{\sigma}{g(\rho_l - \rho_v)} \right]^{-\frac{3}{2}} \quad (3)$$

where Jakob number (Ja) is calculated using equation (4):

$$Ja = \frac{\rho_l c_p l \Delta T_s}{\rho_v \Delta h_v} \quad (4)$$

Jensen and Memmel [6] modified the correlation proposed by Kutateladze and Gogonin [5] as follows:

$$d_{bd} = 0.19 \sqrt{\frac{\sigma}{g(\rho_l - \rho_v)}} (1.8 + 10^5 \cdot C)^{\frac{2}{3}} \quad (5)$$

The fluid properties were calculated at saturation temperature by using [7] in this study as can be seen Table 1:

Table 1 Fluid properties at atmospheric pressure

	FC3284	FC84	FC-mix*
T _s (°C)	50	80	57
M (g/mol)	299	388	321
ρ _l (kg/m ³)	1643	1584	1630
ρ _v (kg/m ³)	10.5	12.5	12.5
C _p (J/kg.K)	1092	1138	1103
μ (Pa.s)	5.34x10 ⁻⁴	4.28x10 ⁻⁴	5.19x10 ⁻⁴
σ (N/m)	0.011	0.008	0.010
k _l (W/mK)	5.85x10 ⁻²	5.34x10 ⁻²	5.72x10 ⁻²
Pr _l	9.97	9.12	10.01

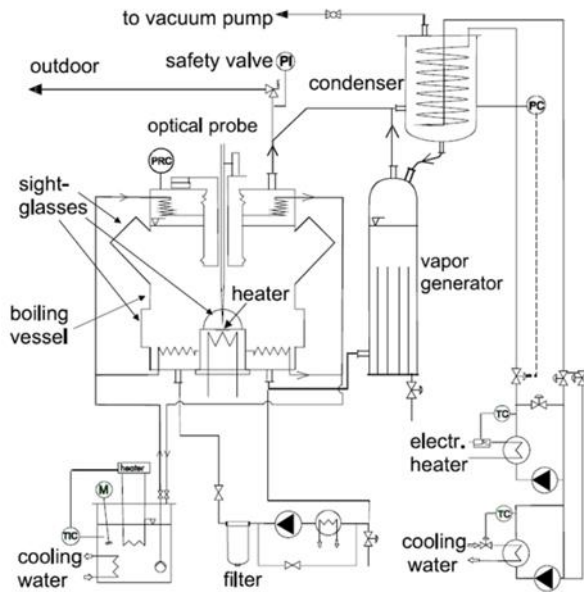
*75 mol% FC3284 – 25 mol% FC84 mixture

Contact angle was assumed 35° for all test substances. Mixture liquid properties were calculated at saturation temperature of mixture with 75% of FC3284 properties and 25% of FC84 properties. However, mixture vapor density was calculated at saturation temperature by using the vapor proportion of the mixture from the previous study of [8].

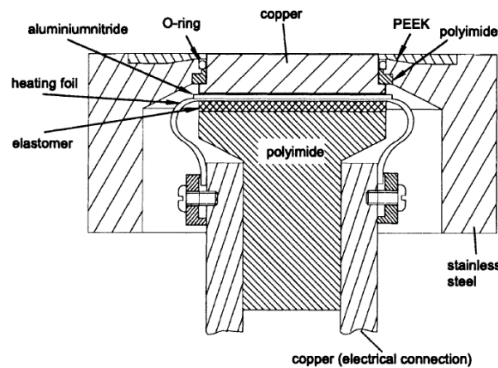
In the study of A. Sathyabhama et al. [9], the Fritz correlation [4] overpredicted the experimental data. It was explained that Fritz correlation [4] was valid only in the region of atmospheric pressure and at low heat flux levels. Also, it was pointed out that Kutateladze and Gogonin [5] and Jensen and Memmel [6] models predict the bubble departure diameter with the weaker function of Jakob number. Therefore, they showed better agreement with the determination of bubble departure diameter. According to S.M. Peyghambarzadeh et al. [10], viscosity has an effect on the various phenomena related to boiling such as bubble formation, bubble growth and detachment, rising velocity from the heating surface. However, most of the correlations (e.g. Fritz correlation) do not take into account the effect of viscosity.

TEST LOOP AND TEST HEATER

Figure 1 depicts a simplified scheme of the test facilities. It has the boiling vessel (diameter 209 mm, height 332 mm), the vapor generator and the condenser as the main components.



(a)



(b)

Figure 1 (a) Test loop and (b) heater section [11]

In order to remove small particles from the test fluid, a filter loop which consists of a heat exchanger, a centrifugal pump and a filter with an absolute removal rating of $0.2 \mu\text{m}$ is used. During the measurements, boiling process is observed through some sightglasses. The system pressure is controlled by the condenser. The vapor generator reheats potentially subcooled liquid from the condenser to preserve constant saturation state at the boiling vessel inlet. The vessel has a test heater at the bottom. The test loop is made from stainless steel, pickled, electropolished and passivated.

The 3D-movable probes which consist of a dual-probe and a micro thermo-probe were installed at the top of the vessel. The dual probe consists of two single mode quartz glass fiber with a diameter of $125 \mu\text{m}$ and a core diameter of $8 \mu\text{m}$. The size of the tip of the probes is less than $1.5 \mu\text{m}$. With this probe, it is possible

to detect vapor and liquid phase by using the different refractive indexes of the phases.

The test heater which is made of copper with a surface diameter of 35 mm and a thickness of 7 mm is fixed in a stainless steel housing. For the prevention of the corrosion and oxidation, the boiling surface is coated with a pure gold layer having a thickness of $1 \mu\text{m}$. A resistance heating foil which provides heat input is pressed on the bottom of the heater. For electrical insulation, the heater has a thin sheet of aluminum nitride ceramic. 14 K-type thermocouples ($\varnothing 0.25 \text{ mm}$) which are used to determine the average surface temperature were implanted in the heater by electroplating. They control temperature and provide protection against overtemperature. In addition to the K-type thermocouples several microthermocouples are implanted in the copper block. A detailed description of the test loop and test heater can be found in [11].

EXPERIMENTAL PROCEDURE

The dual probe was positioned at a distance of 5 mm from the heating surface. The measured signals were conditioned by suitable calculation methods and evaluated using the MATLAB program (Mathworks). With the help of these evaluated data, characteristic quantities such as bubble diameter, bubble velocity and the temperatures inside the bubble can be determined. As an example, Figures 4a and 4b show the measured data of FC3284 with a 0.96 relative heat flux, which is the ratio of the measured heat flux to critical heat flux (CHF) at that moment, in nucleate boiling.

An event corresponds to the time period that the dual-probe stays in a vapor bubble. This time period lasts from the entry of the dual-probe into the vapor bubble to its exit from the vapor bubble. Therefore, an event corresponds to a vapor bubble. In order to display the events better, a million of the measured data is shown in Figure 2a. Since the measurement data was recorded at a frequency of 260 kHz , a measuring point on the abscissa corresponds to $3,846 \times 10^{-6}$ seconds. It is assumed that the vapor bubble is spherical, and its shape does not change during the penetration of the probes and ascent of the bubble in the liquid. The first signal line (upper line) of Figure 2a which is obtained from the micro thermo-probe, represents the temperature profile during measurement time. The second and third lines show respectively the signals of the first and second optical probe in Figure 2a.

Since the first optical probe is on the same level as the micro thermo-probe and the second optical probe is mounted $465 \mu\text{m}$ higher than the other two probes, the signal of the first optical probe generally shows the vapor phase first when compared to second optical probe as shown in Figure 2b. The signals of the micro thermo-probe were not used to determine bubble diameter in this study.

Figure 2b shows the chosen points to determine bubble diameter by focusing on an event. Optical probes are useful to understand whether the phase is liquid or vapor at each measuring point. The lower level of these signal lines indicates the liquid phase while the upper level indicates the vapor phase. The first peak of the first optical probe, "I₁" generally shows the entry into the vapor bubble and the last peak, "O₁" shows the exit

from the vapor bubble while the unnecessary peaks between them are not taken into consideration. Before the first peak, there are fluctuations for some events. For this reason, the beginning of the fluctuations may also present the penetration of the first optical probe into the bubble. So, it was also assumed as the inlet time point (I_0) of the first optical probe. In this case, bubble diameter was determined separately by using two inlet time points (I_0 and I_1) respectively. As a result, the arithmetic mean value of two determined bubble diameters was taken into consideration.

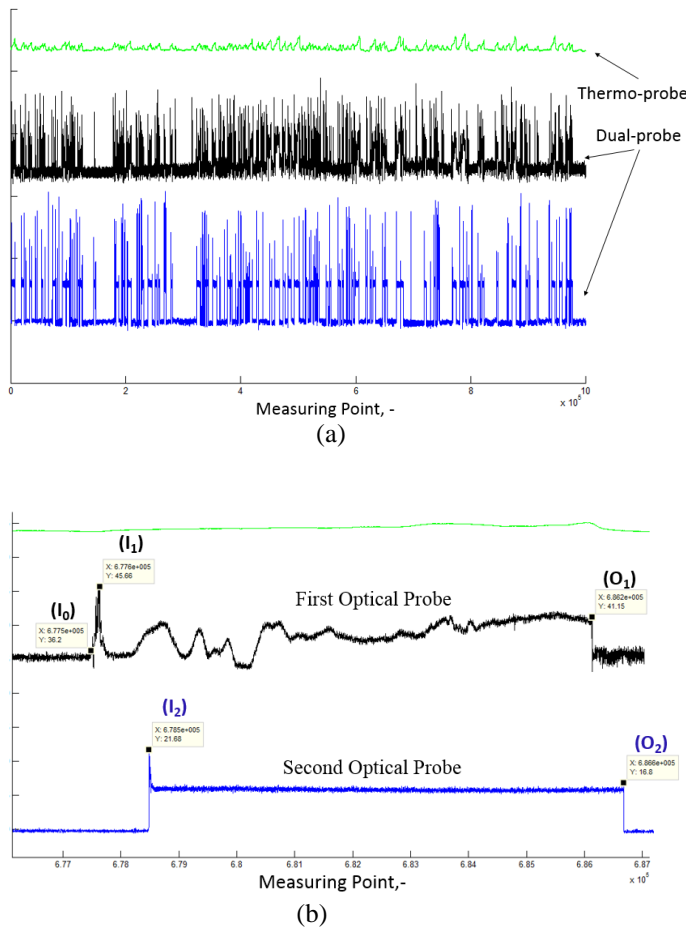


Figure 2 After processing in MATLAB, the signals of the dual-probe with a micro thermo-probe from the measured data of FC3284 with a 0.96 relative heat flux ($q^*=0.96$) in nucleate boiling: (a) all events in a million data; (b) a chosen event

On the other hand, the signal of the second optical probe did not show any significant fluctuation before the first peak point as shown in Figure 2b. Therefore, I_2 is usually taken as the inlet time point of the second optical probe which penetrates into vapor bubble after the first optical probe and “ O_2 ” indicates the exit of the second optical probe.

As seen in the example given in Figure 3, the inlet time difference between the optical probes is greater than the outlet time difference due to spherical form of the vapor bubble. Because, assuming that the vapor bubbles do not accelerate while they rise in the liquid, the first optical probe should stay longer in the vapor bubble than the second optical probe for this example. Therefore, the time period of the first optical probe in the vapor bubble (t_1) will be longer than that of the second optical (t_2). However, this situation could also be opposite if the optical probes penetrated into the vapor bubble from different locations.

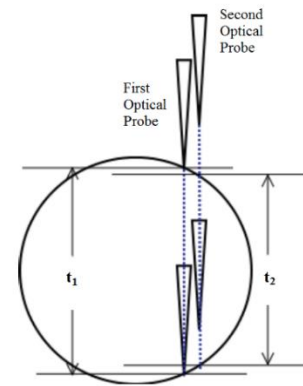


Figure 3 The penetration of the dual-probe into vapor bubble

This is due to the curvature state of the spherical surface of the vapor bubble and the horizontal distance difference ($38 \mu\text{m}$) between the two optical probes. With the help of these inlet and outlet measuring points, bubble velocity and bubble diameter can be evaluated.

Bubble Velocity

Number of measured data (MD) until chosen measuring point can be found by using MATLAB program and actual measuring time (MT) of this point is calculated using equation (6).

$$\frac{\text{Number of MD}}{\text{Recording frequency of MD}} = \text{Actual MT} \quad (6)$$

Inlet and outlet measuring points can be converted to the time values by using equation (6). Then, the inlet and outlet time differences of the optical probes are calculated as followed:

Inlet time differences

$$1) \text{ Relative to } I_0: \Delta t_{\text{inlet}_{2-0}} = (t_{1,2} - t_{1,0}) \quad (7)$$

$$2) \text{ Relative to } I_1: \Delta t_{\text{inlet}_{2-1}} = (t_{1,2} - t_{1,1}) \quad (8)$$

Outlet time difference

$$\Delta t_{\text{outlet}_{2-1}} = (t_{0,2} - t_{0,1}) \quad (9)$$

After calculating the inlet time and outlet time differences of the optical probes, the averaged time value is obtained due to the assumption that the vapor bubble is in spherical form.

1) Relative to I_0 :

$$\Delta t_{\text{average},0} = \frac{(\Delta t_{\text{inlet}_{2-0}} + \Delta t_{\text{outlet}_{2-1}})}{2} \quad (10)$$

2) Relative to I_1 :

$$\Delta t_{\text{average},1} = \frac{(\Delta t_{\text{inlet}_{2-1}} + \Delta t_{\text{outlet}_{2-1}})}{2} \quad (11)$$

Vapor bubble travels from the tip of the first optical probe to the second one during that time period. Thus, velocity can be calculated from each averaged time difference (relative to I_0 and relative to I_1) and the vertical distance which is 465 μm .

$$v_B = \frac{465 \mu\text{m}}{\Delta t_{\text{average}}} \quad (12)$$

As a result two velocity values can be calculated as $v_{B,0}$ and $v_{B,1}$. A detailed description for the calculation of the bubble velocity can be found in [12].

Bubble Diameter

After calculation of bubble velocity, the time period of optical probes in the vapor bubble (t_1 and t_2 in Figure 3) has to be determined. " t_1 " and " t_2 " can be named as the time difference between the inlet and outlet point of the first optical probe and the second optical probe respectively as can be seen from the equations (13) and (14).

$$t_1 = (t_{0,1} - t_{1,1}) \quad (13)$$

$$t_2 = (t_{0,2} - t_{1,2}) \quad (14)$$

The longer time period (t_1 or t_2) is taken to determine the bubble diameter. Because the optical probe which is closer to the center of the bubble, stay longer in the bubble.

Therefore, the two bubble diameters can be calculated from the two bubble velocities which are $v_{B,0}$ and $v_{B,1}$ and the longer time period of the optical probes in the bubble;

$$d_{B,0} = v_{B,0} \times (t_1 \text{ or } t_2) \quad (15)$$

$$d_{B,1} = v_{B,1} \times (t_1 \text{ or } t_2) \quad (16)$$

RESULTS AND DISCUSSION

For the determination of the bubble diameter, the measurements were carried out by using the test substances FC3284, FC84 and their binary mixtures which include 50 mol% and 75 mol% of FC3284 at atmospheric pressure in whole boiling region.

Determination of mean bubble diameter

Diameters of the vapor bubbles which were calculated by using equation (16) and their arithmetic mean are shown for pure substances and their binary mixtures with the different relative heat fluxes in nucleate boiling region in Figure 4. At least one million measured data were examined and the events which show clearly existing bubbles are taken into consideration.

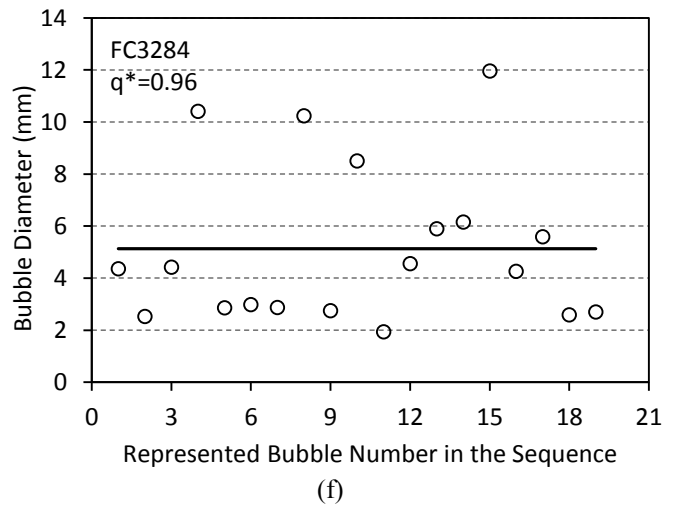
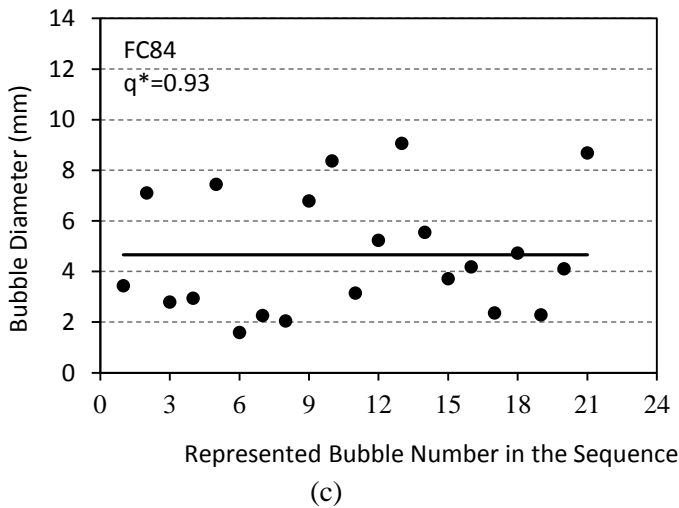
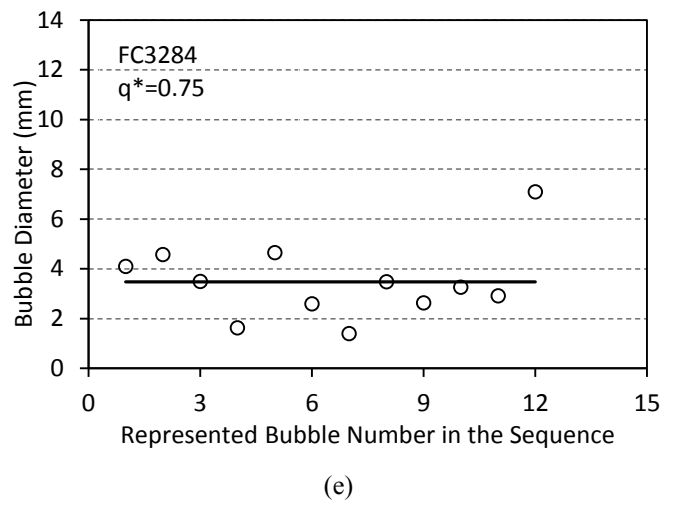
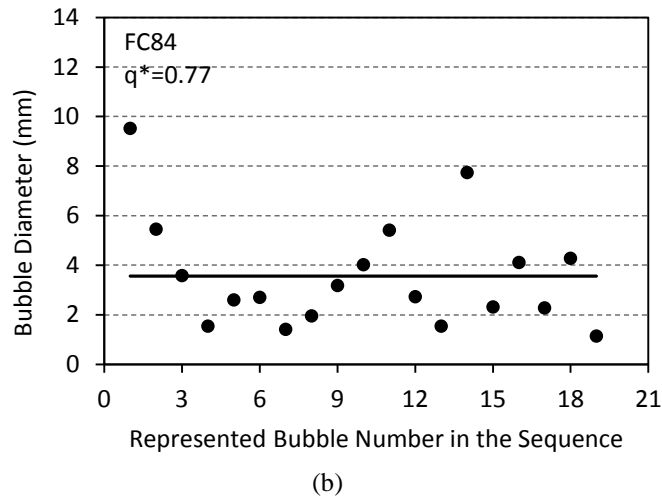
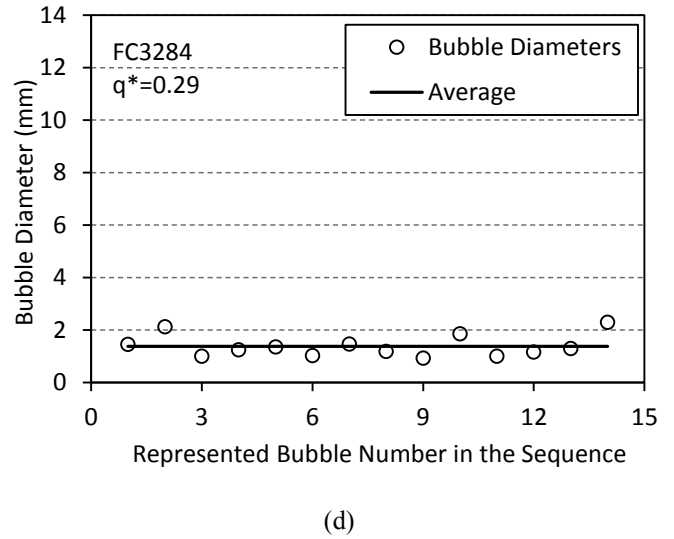
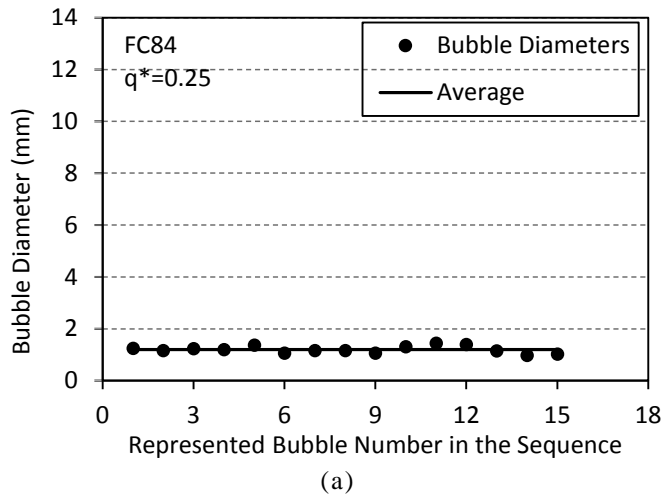


Figure 4 Measured bubble diameters ($d_{b,1}$) and their arithmetic mean relative to the heat flux in nucleate boiling for FC84 and FC3284 respectively at atmospheric pressure

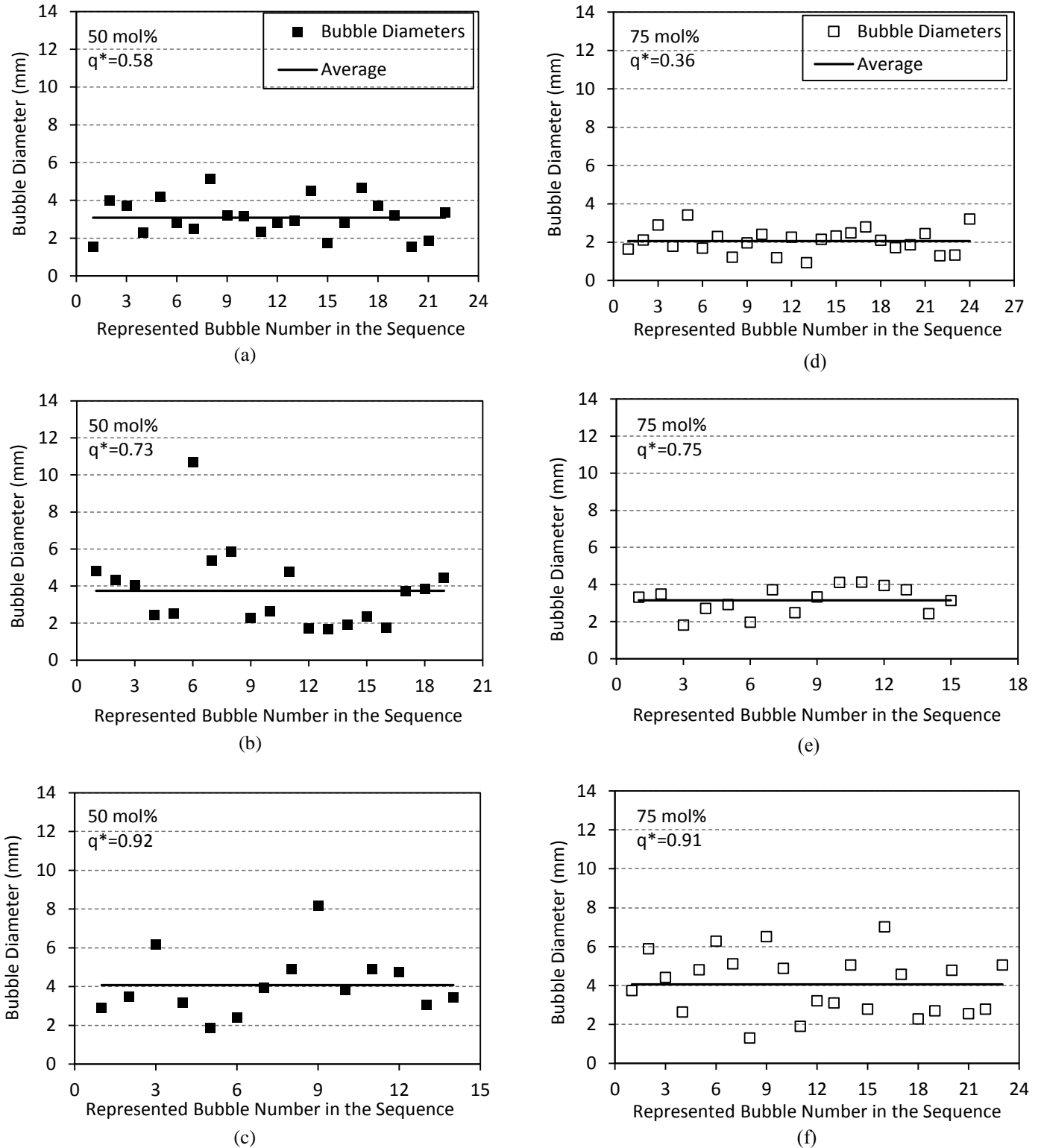


Figure 5 Measured bubble diameters ($d_{b,1}$) and their arithmetic mean relative to the heat flux for the mixtures of 50 mol% and 75 mol% of FC3284 respectively in nucleate boiling at atmospheric pressure

At the beginning of nucleate boiling the measured bubble diameters showed low variations for both FC84 and FC3284 (Figures 4a and 4d). However, the variation of the measured bubble diameters increased at higher relative heat fluxes in nucleate boiling as shown in Figures 4b and 4c for FC84, in Figures 4e and 4f for FC3284. Bubble dynamics between the heating surface and the dual-probe may be greater at high heat flux than that at low heat flux. Therefore, vapor bubbles may be affected from each other and from the liquid conditions around the vapor bubble in nucleate boiling. Additionally, sometimes the dual-probe was not able to contact with the bubble at its centerline, as a result the dual-probe's measurements of the diameter were lower than the real one.

The measured bubble diameters are shown for mixtures of FC3284 and FC84 in Figure 5. In comparison with the pure substances, bubble diameter variations are higher for the mixtures at the beginning of the nucleate boiling. However, the variations of the measured bubble diameters are not as much as for the pure substances at higher relative heat fluxes. It was determined that bubble formation of the mixtures starts at higher relative heat flux. That is why measured bubble diameters may be larger than those of the pure substances. However, the mean bubble diameters at high relative heat flux for the mixtures were smaller than that of the pure substances in the nucleate boiling as shown in Figure 5.

The mean bubble diameter in different boiling regions

As an example, the arithmetic mean of the $d_{b,0}$ and $d_{b,1}$ for the test substance FC3284 are shown with the wall superheat and relative heat flux in Figure 6.

For every arithmetic mean bubble diameter, $d_{b,1}$ and $d_{b,0}$ were shown as maximum and minimum diameters respectively in Figure 6. Wall superheat is obtained by the subtraction of the saturation temperature (T_s) from the actual heating wall temperature (T_w). Relative heat flux is defined as the ratio of the measured heat flux to the critical heat flux in the boiling curve.

As shown in Figure 6, bubble diameter increases with increasing wall superheat in nucleate boiling region. At critical heat flux, bubble diameter started to decrease. In the transition boiling region, the measured bubble diameter was as large as it can be at the critical heat flux. In the film boiling region, the bubble diameter was smaller than that of the one in the transition boiling region because the dual-probe measured only the vertical distance and there is not a spherical formation of the bubbles which detach from the vapor film on the heating surface in the film boiling.

The comparison of the bubble diameters for FC3284, FC84, 50 mol% mixture, 75 mol% FC3284 - 25 mol% FC84 mixture is shown with the wall superheat in Figure 7.

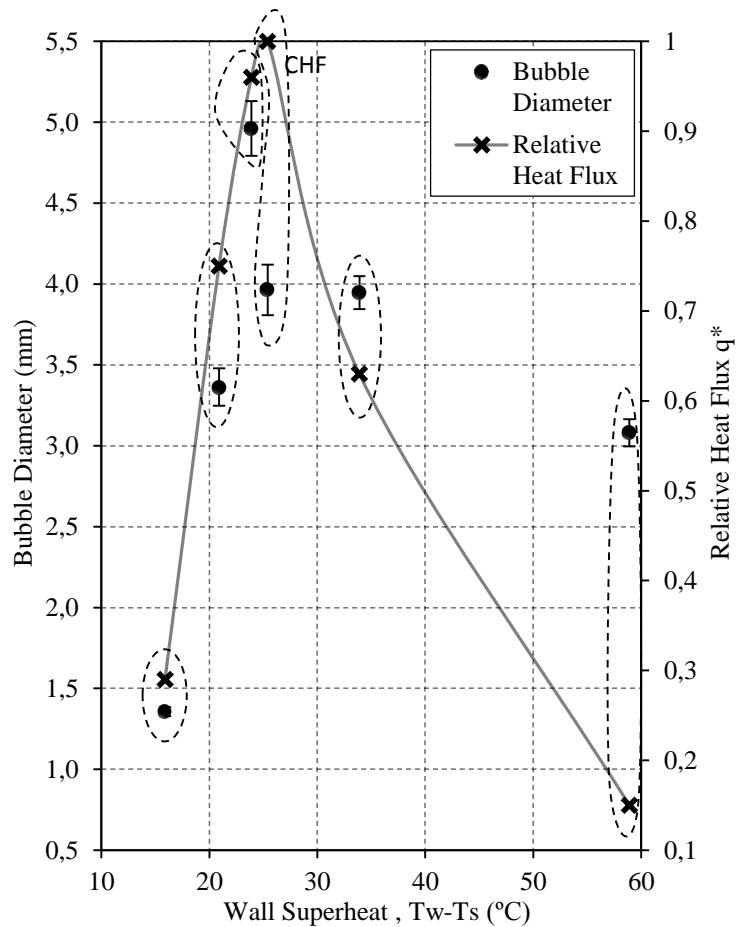


Figure 6 Arithmetic mean of the $d_{b,0}$ and $d_{b,1}$ for FC3284 versus wall superheat and relative heat flux.

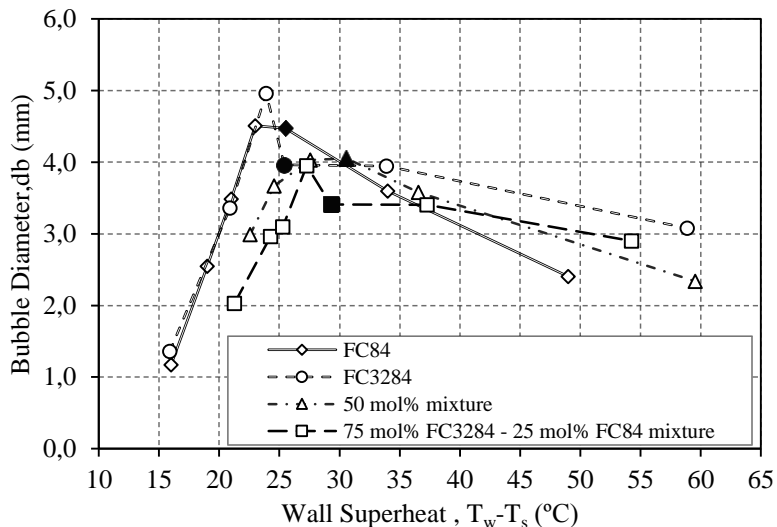


Figure 7 Arithmetic mean of the $d_{b,0}$ and $d_{b,1}$ for the test substances FC3284, FC84, 50 mol% mixture, 75 mol% FC3284 - 25 mol% FC84 mixture versus wall superheat.

The trends of the bubble diameters with the wall superheat show the difference between the pure substances. Namely, the bubble diameter of FC3284 shows a peak value near the critical heat flux (CHF) whereas there is almost the same bubble diameter near and at the CHF for FC84. Bold marks show the bubble diameters at CHF for pure and mixtures. A mixture of 75 mol% FC3284 - 25 mol% FC84 showed the same tendency as the pure substance FC3284 did with the wall superheat. However a mixture of 50 mol% FC3284 - 50 mol% FC84 has the same tendency as the pure substance FC84 as shown in Figure 7.

Comparison of the mean bubble diameter with the correlations

Figure 8 shows a comparison of measured bubble diameters with the values of correlations according to Fritz [4], Kutateladze and Gogonin [5] and Jensen and Memmel [6]. The result of 50 mol% mixture was not shown in Figure 8, because bubble formation for this mixture begins at higher relative heat flux.

From the previous study of [12], the results of FC3284 are in agreement with the correlation results shown in Figure 8. It was used 5 mm distance from the heating surface for a relative heat flux which was 0.12 at the beginning of the nucleate boiling. The correlations of Jensen and Memmel [6] and Kutateladze and Gogonin [5] showed a better result than that of Fritz [4]. They both include the effect of wall superheat and viscosity which are not taken into account in Fritz [4]. These correlations are valid for the departure diameter. On the other hand, the difference between the correlation results and measured results increases at higher heat fluxes in nucleate boiling as can be seen in Figure 8. Since all the nucleation sites were waited to be activated in the measurements, bubbles were started to be measured at a relative heat flux higher than 0.12 which was examined as the beginning of the nucleate boiling by [12]. At higher relative heat flux in nucleate boiling, bubbles may influence each other which are not taken into account in the correlations. Furthermore the correlations of Jensen and Memmel [6] and Kutateladze and Gogonin [5] may not show the effect of the wall superheat sufficiently as A. Sathyabhama et al. [9]'s study reported. Therefore, all of the presented measured results are higher than the correlation results for the pure substances and the mixture of 75 mol% FC3284 as shown in the Figure 8. For the pure substances FC3284 and FC84, the measured results are approximately two times higher than the correlation results.

As can be seen from Figure 8, in comparing the three correlations to one another, there is no significant difference. Without taking into account the effect of viscosity, the correlation of Fritz [4] shows a satisfying result.

For the binary mixture of FC3284 and FC84 which includes 75 mol% FC3284, measured result and correlation results shows greatest difference. This is because of the fact that the mixture effect, which causes nucleate boiling to start at higher wall superheats, was not taken into consideration in the correlations.

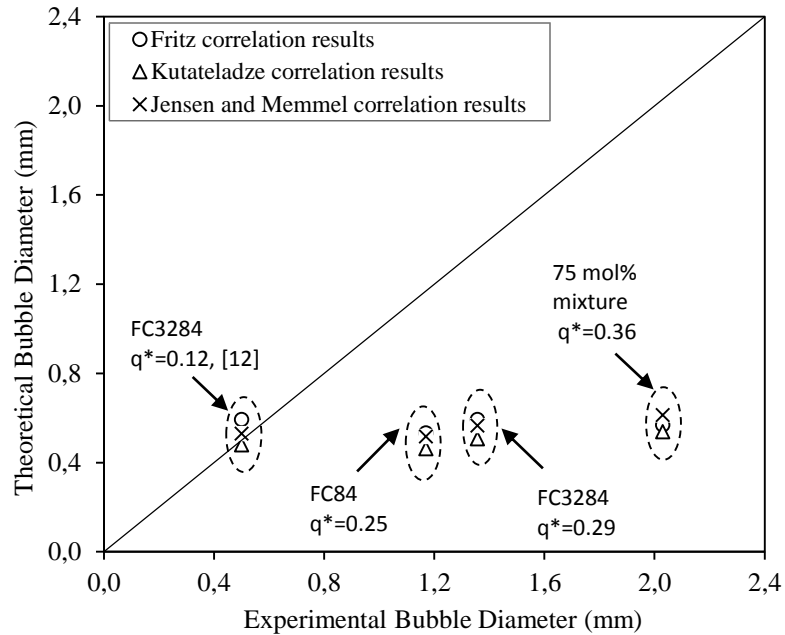


Figure 8 Comparison of the measured bubble diameter with predictions from the correlations for low relative heat flux in nucleate boiling at atmospheric pressure

CONCLUSION

Bubble diameter was investigated experimentally by using FC3284, FC84 and their binary mixtures which includes 50 mol% and 75 mol% of FC3284 at atmospheric pressure in whole boiling region.

For all test substances, bubble diameters increase with increasing wall superheat and the variation of bubble diameters increases at high relative heat fluxes in nucleate boiling region. Two different trends were observed: For FC3284 and 75 mol% of FC3284 binary mixture, bubble diameters decreased at CHF. However for FC84 and 50 mol% of FC84 binary mixture, bubble diameters did not change at CHF.

The fluctuations of the first optical probe signals which was observed during the penetration into the bubble, did not show any important difference in the results of bubble diameter determination.

The arithmetic means of the measured bubbles were compared to the correlations of Fritz [4], Kutateladze and Gogonin [5] and Jensen and Memmel [6]. It was found that the correlation results showed good agreement with the result of FC3284 in [12] at the beginning of nucleate boiling.

At higher relative heat flux, there was a big difference between the results of correlations and measured bubble diameters.

The effect of wall superheat was not observed in the correlations. As a result there was a great difference between theoretical and experimental results at higher relative heat fluxes in nucleate boiling.

ACKNOWLEDGEMENTS

The authors highly appreciate financial support of Deutsche Forschungsgemeinschaft (DFG) in the frame of a Joint Research Project on fundamentals of boiling heat transfer.

REFERENCES

- [1] S. Hamzekhani, M. Maniavi Falahieh, A. Akbari, Bubble departure diameter in nucleate pool boiling at saturation: Pure liquids and binary mixtures, *International Journal of Refrigeration* 46 (2014), pp. 50-58
- [2] H. Sakashita, A. Ono, Y. Nakabayashi, Measurements of critical heat flux and liquid–vapor structure near the heating surface in pool boiling of 2-propanol/water mixtures, *International Journal of Heat and Mass Transfer* 53 (2010) 1554–1562
- [3] E. Wagner, A. Sprenger, P. Stephan, O. Koeppen, F. Ziegler, and H. Auracher, Nucleate Boiling at Single Artificial Cavities: Bubble Dynamics and Local Temperature Measurements, *Sixth International Conference on Multiphase Flow ICMF 2007*.
- [4] W. Fritz, Berechnung des Maximalvolumens von Dampfblasen. *Phys.*, 1935, pp. 36:379–388
- [5] S.S. Kutateladze, I.I. Gogonin, Growth rate and detachment diameter of a vapor bubble in free convection boiling of a saturated liquid, *High Temp.* 17, 1979, pp. 667–671
- [6] M.K. Jensen, G.J. Memmel, Evaluation of bubble departure diameter correlation, in: *Proc. Eighth Int. Heat Transfer Conf.*, vol. 4, 1986, pp. 1907– 1912
- [7] 3M GmbH. Product information on FC3284 and FC84 fluorinerts:
<http://multimedia.3m.com/mws/media/648870/fluorinert-electronic-liquid-fc-3284.pdf>
<http://multimedia.3m.com/mws/media/648950/fluorinert-electronic-liquid-fc-84.pdf>
<http://multimedia.3m.com/mws/media/654950/3mtm-thermal-management-fluids.pdf>
- [8] D. I. Kluge, Untersuchung des Gemisches FC3284/FC84 beim Behältersieden mit Hilfe eines temperaturgeregelten Heizers. *Bachelorarbeit, Institut für Energietechnik, TU Berlin, 2013*
- [9] A. Sathyabhama, T. P. Ashok Babu, Nucleate Pool Boiling Heat Transfer Measurement and Flow Visualization for Ammonia-Water Mixture, *Journal of Heat Transfer, ASME Publication, 133(10), 101506, October 2011*
- [10] S.M. Peyghambarzadeh, A. Hatami, A. Ebrahimi, S.A. Alavi Fazel, Photographic study of bubble departure diameter in saturated pool boiling to electrolyte solutions, 2012. *Chem. Ind. Chem. Eng. Q.* 1,120
- [11] M. Buchholz, Lokale Mechanismen des Wärmeübergangs beim Behältersieden in allen Bereichen der Siedekennlinie, *Dissertation, TU Berlin, 2005*
- [12] O. Koeppen, Analyse von Siedezuständen an einer Heizfläche mit optischen Mehrfachsonden. *Diplomarbeit, Institut für Energietechnik, TU Berlin, 2004*